OPTICAL BEAM QUALITY IN FREE-ELECTRON LASERS *

P. Sprangle[1], H.P. Freund[2], B. Hafizi[3], and J.R. Peñano[1]
[1]Plasma Physics Division of the Naval Research Laboratory, Washington, DC 20375, U.S.A.
[2]Science Applications International Corporation, 1710 SAIC Drive, McLean, VA 22102, U.S.A.
[3]Icarus Research Inc., P.O. Box 30780, Bethesda, MD 20824-0780, U.S.A.

Abstract

The mode quality of free-electron lasers (FELs) is near the diffraction limit. Here, we analyze the optical mode quality in FELs using the M^2 parameter, which is a measure of the size and divergence of the optical beam. We calculate M^2 in two ways: (1) by a direct integration over the transverse mode structure, and (2) by allowing the mode to expand beyond the wiggler and analyzing the divergence. A numerical analysis is conducted using the MEDUSA simulation code that shows that M^2, as expected, is near unity at saturation.

INTRODUCTION

It is widely known that the mode quality of the output of free-electron lasers (FEL) is near the diffraction limit [1-3]. Good optical beam quality is important in many FEL applications. In particular, it is relevant to atmospheric propagation of high power FELs [4,5] as well as to the application of FELs in research environments at ultraviolet and x-ray wavelengths [6-9]. Numerical analysis has shown that the mode content in an FEL oscillator is predominantly in the TEM_{00} mode for oscillators that use transmissive outcoupling [1]. The optical mode quality was observed in the Los Alamos FEL oscillator [2,3] where the mode was shown to be near the diffraction limit. The mode quality in this experiment was characterized by a measurement of the Strehl ratio [10], which is defined in the far field as the ratio of the on-axis intensity to the intensity of a pure Gaussian mode (TEM_{00}) with the same spot size. As such, the Strehl ratio has a maximum value of unity for an ideal, pure Gaussian beam and decreases as the higher order mode content increases. The Strehl ratio was found to be approximately 0.9 in the Los Alamos oscillator indicating an output mode close to a pure Gaussian. However, the Strehl ratio is difficult to determine for optical modes that differ appreciably from that of a Gaussian. Higher order mode content is likely to be more important in single-pass FELs, such as Master Oscillator Power Amplifiers (MOPA) or Self-Amplified Spontaneous Emission (SASE) configurations that are operated past saturation.

The beam quality in FELs can be quantified by means of the M^2 parameter [11-13], which is a measure of the higher order mode content in the optical beam. It is equal to unity for a perfect Gaussian beam (pure TEM_{00}) and increases as the mode quality deteriorates, i.e., the divergence angle of the beam increases as the higher order mode content increases. Thus, the divergence angle of an optical beam is often described as "times diffraction limited" in the far field, where the term "times diffraction limited" is relative to the spreading angle of a fundamental Gaussian mode with an equivalent spot size. The M^2 parameter is analogous to emittance, which is a measure of beam quality in particle beams. M^2 was measured in the FEL oscillator experiment at Thomas Jefferson National Accelerator Facility [14]. This experiment produced average powers in excess of 2 kW at a wavelength of 3.1 microns. Measurements indicated a nearly pure fundamental Gaussian mode with M^2 = 1.1 at the output mirror for powers up to about 350 W. As the power increased beyond 350 W, M^2 increased and reached values of ~ 2 for powers of 500 W. However, much of the increase in M^2 that occurred at higher power levels was attributed to mirror distortions and not the wave-particle interaction in the FEL. As a result, the mode quality may be improved in high-power oscillators using mirrors that compensate for distortions. It should also be remarked that the mode quality in high-power amplifiers is governed solely by the FEL interaction.

In this paper we examine the mode quality in FEL amplifiers and determine M^2 in two ways: (1) by a direct integration over the transverse mode structure, and (2) by allowing the mode to expand beyond the wiggler and analyzing the mode divergence as discussed in Sec. II. In Sec. III we study M^2 in FEL amplifiers using the MEDUSA simulation code [15,16].

THE M^2 PARAMETER

The spot size of an axially symmetric laser beam is defined to be

$$W^2(z) = 2\frac{\iint dxdy r^2 I(x,y,z)}{\iint dxdy I(x,y,z)}. \qquad (1)$$

where $I(x,y,z)$ is the time-averaged intensity, which can contain higher order modes. In the paraxial approximation, it can be shown that in a linear, homogeneous medium, the spot size evolves according to the parabolic propagation rule [10-13]

$$W^2(z) = W_0^2 + M^4\frac{\lambda^2}{\pi^2 W_0^2}(z-z_0)^2 \qquad (2)$$

where λ is the laser wavelength and z_0 is the location of the waist, and W_0 is the spot size at the waist. From Eq.

*Work supported by the Joint Technolgy Office and the Office of Naval Research in the USA.
[1]sprangle@ppd.nrl.navy.mil

(2), the asymptotic divergence angle is given by $\theta_D = M^2\lambda/(\pi W_0)$, as shown schematically in Fig. 1.

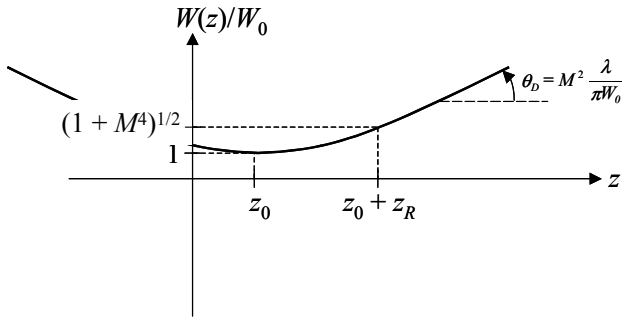

Figure 1: Schematic illustration of parabolic mode expansion.

In deriving an expression for M^2, we represent the optical mode in the form, $\boldsymbol{E}(\boldsymbol{x},t) = (1/2)A(\boldsymbol{x})\,\hat{\mathbf{e}}_\perp \exp(ikz - i\omega t) + c.c.$, where $A(\boldsymbol{x})$ is the complex field amplitude, $k = \omega/c$, ω is the angular frequency, $\hat{\mathbf{e}}_\perp$ is a unit vector in the transverse direction that defines the polarization of the field, and *c.c.* denotes the complex conjugate. The complex field amplitude can be written as a superposition of Gauss-Hermite modes

$$A(\mathbf{x}) = \sum_{m,n=0}^{\infty} A_{m,n} w(0) U_m(x,z) U_n(y,z) \times \exp\left[i\theta_{m,n}(z)\right]\exp\left[-i\alpha(z)r^2/w^2(z)\right], \quad (3)$$

where $A_{m,n}$ are constants,

$$U_m(x,z) = \left(\frac{2}{\pi}\right)^{1/4} \frac{1}{\sqrt{2^m m! w(z)}} \times H_m\left(\frac{\sqrt{2}x}{w(z)}\right)\exp\left(-x^2/w^2(z)\right), \quad (4)$$

and H_m denotes the Hermite polynomial of order m [17]. The complex field amplitude must satisfy the free space paraxial wave equation, $[\nabla_\perp^2 + 2ik(\partial/\partial z)]A = 0$, so that

$$\alpha(z) = \alpha(0) - \left[1 + \alpha^2(0)\right]\frac{z}{z_R}, \quad (5a)$$

$$w^2(z) = w^2(0)\left\{1 + \left[1 + \alpha^2(0)\right]\frac{z^2}{z_R^2} - 2\alpha(0)\frac{z}{z_R}\right\}, \quad (5b)$$

and

$$\theta_{m,n} = (m + n + 1)[\tan^{-1}\alpha(z) - \tan^{-1}\alpha(0)], \quad (5c)$$

where α denotes the radius of curvature, and $\theta_{m,n}$ is the generalized Guoy phase. The initial values of α and w are, in general, arbitrary but should be chosen judiciously in order to minimize the number of modes necessary to characterize the field. The quantity $w(z)$ denotes the spot size of the fundamental (TEM_{00}) Gaussian mode, $z_R = \pi w^2(0)/\lambda$ is the Rayleigh range with respect to the Gaussian spot size at $z = 0$.

Free space propagation is assumed in this field representation. As such, it does not represent the evolution of the field within the wiggler in an FEL. Rather, the $z = 0$ position denotes the field at the exit of the wiggler, at which point the complex field amplitudes can be expressed as

$$A_{m,n} = \frac{1}{w(0)}\int_{-\infty}^{\infty} dx \int_{-\infty}^{\infty} dy A(x,y,0)U_m(x,0)U_n(y,0) \times \exp\left(i\alpha(0)r^2/w^2(0)\right). \quad (6)$$

The field amplitudes at the wiggler exit are used to determine M^2.

The optical intensity is given by

$$I(x,y,z) = \frac{c}{8\pi}A(x,y,z)A^*(x,y,z) = \frac{c}{8\pi}w^2(0)\sum_{m,m',n,n'} A_{m,n}A^*_{m',n'}U_m(x,z)U_{m'}(x,z) \times U_n(y,z)U_{n'}(y,z)\exp\left[i\theta_{m,n}(z) - i\theta_{m',n'}(z)\right], \quad (7)$$

and the total power is constant and given by

$$P_0 = \int_{-\infty}^{\infty} dx \int_{-\infty}^{\infty} dy\, I(x,y,z) = \frac{c}{8\pi}w^2(0)\sum_{m,n} A_{m,n}A^*_{m,n}. \quad (8)$$

The spot size for a symmetric beam follows from Eq. (1) and is

$$W^2(z) = w^2(z)\frac{\sum_{m,n}(2m+1)A_{m,n}A^*_{m,n}}{\sum_{m,n}A_{m,n}A^*_{m,n}} + 2w^2(0)\left[1 - \left(1 - \alpha^2(0)\right)\frac{z^2}{z_R^2} - 2\alpha(0)\frac{z}{z_R}\right] \times \frac{\sum_{m,n}\sqrt{(m+1)(m+2)}A_{m,n}A^*_{m+2,n}}{\sum_{m,n}A_{m,n}A^*_{m,n}}, \quad (9)$$

Since the initial phases between the modes are uncorrelated and vary randomly in time, we can perform a time average of Eq. (9) so that the off-diagonal terms vanish, and we obtain

$$W^2(z) = \frac{c\,w^2(0)\,w^2(z)}{8\pi P_o}\sum_{m,n}(2m+1)A_{m,n}A^*_{m,n} = \frac{W^2(0)}{w^2(0)}w^2(z). \quad (10)$$

The optical beam quality factor M^2 can be written in terms of the complex mode amplitudes, $A_{m,n}$. For a collimated beam, $\alpha_0(0) = 0$, the square of the spot size in Eq.(10) becomes $W^2(z) = W^2(0)(1 + z^2/z_R{}^2)$. Comparing this result with Eq. (2) for a collimated beam, we find that $M^2 = (\pi W^2(0)/\lambda)/z_R = W^2(0)/w^2(0)$. Substituting this into Eq.(10), yields the beam quality factor in terms of the mode amplitudes,

$$M^2 = \frac{cw^2(0)}{8\pi P_0}\sum_{m,n}(2m+1)A_{m,n}A^*_{m,n}. \quad (11)$$

If the modal decomposition at the exit of the wiggler in an FEL is known, i.e., mode amplitudes, spot size w and curvature α, M^2 can be calculated for the output optical mode using Eq. (11). However, if there is significant higher order mode content, then the convergence of the technique will depend upon an accurate determination of these higher order modes. Therefore, it is useful to have an alternate technique for obtaining M^2. One such technique, based on the parabolic propagation rule, makes use of the expansion of the optical mode. The spot size of the beam is calculated using Eq. (1) at three different axial positions after the wiggler exit and is used in Eq. (2) to obtain the three unknowns, W_0, z_0, and M^2.

NUMERICAL ANALYSIS

For simulation purposes, we use the 3-D FEL simulation code MEDUSA [15,16] which can model planar or helical wiggler geometry, treats the electromagnetic field as a superposition of Gaussian modes (Hermite or Laguerre). The code uses an adaptive eigenmode algorithm called the Source-Dependent Expansion [18] to self-consistently describe the guiding of the optical mode through the wiggler. The field equations are integrated simultaneously with the 3-D Lorentz force equations for an ensemble of electrons. No wiggler-average orbit approximation is used, and MEDUSA can propagate the electron beam through a complex wiggler/transport line including multiple wiggler sections, quadrupole and dipole corrector magnets, FODO lattices, and magnetic chicanes. In addition, MEDUSA can propagate the field beyond the exit from the wiggler in free space. Both of the techniques described above to determine M^2 can be simulated using MEDUSA, *i.e.*, (i) obtaining the mode amplitudes at the end of the wiggler and performing the modal sum in Eq. (11) and (ii) propagating the field beyond the wiggler exit and determining the spot sizes at three different axial points which, from Eq. (2), yields M^2.

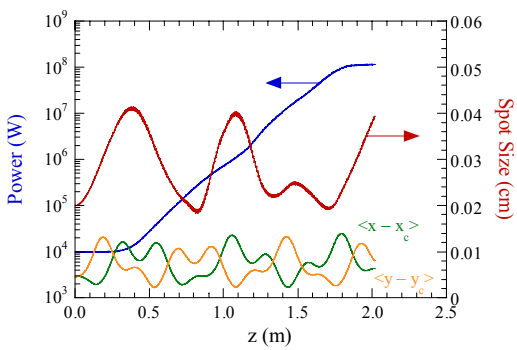

Figure 2: Evolution of the power, spot size and beam envelopes in the x- and y-directions.

The example under consideration is that of a seeded amplifier at a wavelength of 0.8 μm that utilizes a strong-focusing wiggler. The wiggler modeled is the VISA wiggler [19] in which the focusing quadrupoles are incorporated into the wiggler design. The electron beam has an energy of 72.5 MeV and a peak current of 300 A. The emittance and energy spread are 2.0 mm-mrad and 0.01% respectively. The initial beam size in the x-and y-directions is 46 μm, and the Twiss-α parameter is zero. It should be remarked that no attempt has been made to produce an ideal match into the FODO lattice. The wiggler period is 1.8 cm and the maximum on-axis field strength is 7.5 kG with a field error of 0.4% and a gap of 6.0 mm. The FODO cells have a length of 24.75 cm and each quadrupole has a length of 9.0 cm and a focusing gradient of 33.3 T/m. Hence, the separation between quadrupoles is 12.38 cm.

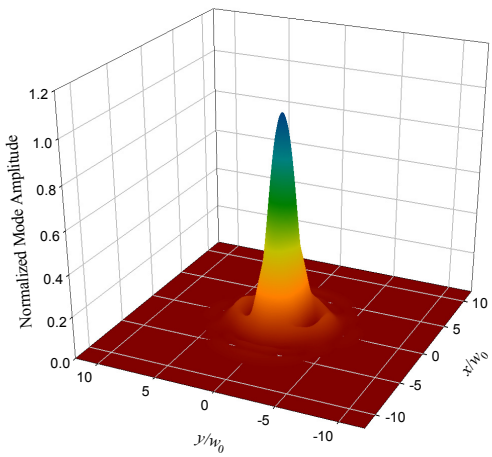

Figure 3. Transverse mode pattern at the wiggler exit for a seed power of 10 kW.

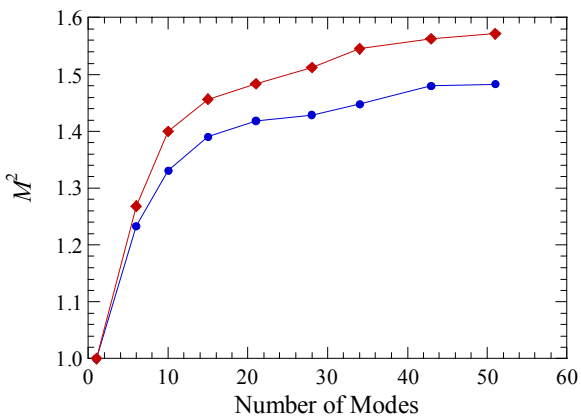

Figure 4. Variation in M^2 versus the number of modes included in the simulation showing convergence after about 40 modes.

The first case we consider makes use of 34 Gauss-Hermite modes and assumes a seed power of 10 kW. This yields saturation at the end of the wiggler at a power level of 115 MW. The evolution of the power, overall spot size of the optical mode, and the beam envelopes in the x- and y-directions is shown in Fig. 2. Observe that the beam envelopes in the x- and y-directions vary as expected in the FODO lattice and that the overall mode spot size expands and contracts with the beam envelope showing the optical guiding of the radiation; however, the guiding is

not strong enough for the optical mode to follow all the variations in the beam envelope. The use of 34 modes in the simulation means that very high order modes are included. Propagating this field beyond the exit of the wiggler, we find that $M^2 = 1.45$, which is close to the diffraction limit as expected in FELs and corresponds to a near-Gaussian mode pattern as shown in a normalized transverse mode pattern in Fig. 3.

An important issue in modeling the beam quality in FELs using the modal decomposition at the exit from the wiggler is the convergence of M^2 with respect to the number of modes in the superposition. The number of modes required to obtain reasonable values for the saturated power is generally smaller than that required to obtain an accurate determination of the optical mode quality as measured by M^2. This is because the FEL preferentially excites lower order Gaussian modes. However, the effect of the higher order modes is enhanced in the determination of M^2 as shown in Eq. (11) where the modal sum is weighted by the factor $(2m + 1)$ that gives higher weights for the higher order modes. For example, simulation using 6 Gauss-Hermite modes also yields a saturated power of 115 MW which is the same power found using 34 modes, but $M^2 = 1.23$. Hence, it is important to determine the number of modes required to reach convergence. This is shown in Fig. 4 for these parameters where we plot M^2 versus the number of Gauss-Hermite modes in the superposition using both the analytic, Eq. (11), and propagation methods. It is clear from the figure that convergence is achieved using ~ 40 modes for $M^2 = 1.48$ using the propagation method. The analytic method converges to a value of $M^2 = 1.57$ for a discrepancy of about 5.5%. We attribute this discrepancy between the analytic and propagation methods to the fact that the analytic method was derived under the assumption of axially symmetric optical modes, while the actual mode displays a small degree of asymmetry.

SUMMARY AND DISCUSSION

In summary, we have discussed the determination of optical beam quality, *i.e.*, M^2, in FELs by two methods. One is a direct calculation based on the mode decomposition at the end of the wiggler and the other relies on a three-point fit to the optical mode spot size as it propagates beyond the end of the wiggler. We found that the simulation required a relatively large number of higher order modes to achieve convergence in the determination of M^2. The results indicate that the beam quality to be expected is near-diffraction limited when the wiggler length is comparable to the saturation length. For wigglers longer than the saturation length, however, higher order mode content increases and the optical mode quality decreases (M^2 increases).

REFERENCES

[1] D.C. Quimby and J. Slater, IEEE J. Quantum Electron. **QE-19**, 800 (1983).

[2] B.E. Newnam *et al*., IEEE J. Quantum Electron. **QE-21**, 867 (1985).

[3] B.E. Newnam *et al*., Nucl. Instrum. Meth. **A237**, 187 (1985).

[4] P. Sprangle *et al*., IEEE J. Quantum Electron. **40**, 1739 (2004).

[5] P. Sprangle *et al*., J. Directed Energy **2**, 71 (2006).

[6] S. Krinsky and L.H. Yu, Phys. Rev. A 35, 3406 (1987).

[7] K.J. Kim, "Temporal and Transverse Coherence of SASE," in *Towards x-Ray Free-Electron Lasers*, eds. R. Bonifacio and W. Barletta, (AIP Conference Proceedings No. 413, 1997), p.3.

[8] E. Saldin *et al*., The Physics of Free Electron Lasers (Springer, Berlin, 1999).

[9] M. Xie, Nucl. Instrum. Meth. **A445**, 67 (2000).

[10] M. Born and E. Wolf, *Principles of Optics: Electromagnetic Theory of Propagation, Interference, and Diffraction of Light*, (Cambridge University Press, Cambridge, England, 1999).

[11] A.E. Siegman, Proc. Soc. Photo-Opt. Instrum. Eng. **1224**, 2 (1990).

[12] T.F. Johnson, Jr., Laser Focus World **26**, 173 (1990).

[13] A.E. Siegman, IEEE J. Quantum Electron. **27**, 1146 (1991).

[14] S.V. Benson *et al*., Nucl. Instrum. Meth. **A483**, 434 (2002).

[15] H.P. Freund *et al*., IEEE J. Quantum Electron. **36**, 275 (2000).

[16] H.P. Freund, Phys. Rev. ST-AB **8**, 110701 (2005).

[17] A.E. Siegman, *Lasers* (University Science Books, Mill Valley, CA, 1986).

[18] P. Sprangle *et al*., Phys. Rev. A **36**, 2773 (1987).

[19] R. Carr *et al*., Phys. Rev. **ST-AB**, 4, 122402 (2001).